Philosophical Magazine

ISSN: 1478-6435 (Print) 1478-6443 (Online) Journal homepage: http://www.tandfonline.com/loi/tphm20

Effect of temperature-dependent surface heat transfer coefficient on the maximum surface stress in ceramics during quenching

Y. F. Shao, F. Song, C. P. Jiang, X. H. Xu, J. C. Wei & Z. L. Zhou

To cite this article: Y. F. Shao, F. Song, C. P. Jiang, X. H. Xu, J. C. Wei & Z. L. Zhou (2016) Effect of temperature-dependent surface heat transfer coefficient on the maximum surface stress in ceramics during quenching, Philosophical Magazine, 96:4, 387-398, DOI: 10.1080/14786435.2015.1134836

To link to this article: http://dx.doi.org/10.1080/14786435.2015.1134836

Published online: 25 Jan 2016.

PHILOSOPHICAL MAGAZINE, 2016
VOL. 96, NO. 4, 387–398
http://dx.doi.org/10.1080/14786435.2015.1134836

Taylor & Francis
Taylor & Francis Group

Effect of temperature-dependent surface heat transfer coefficient on the maximum surface stress in ceramics during quenching

Y. F. Shao[a], F. Song[a], C. P. Jiang[a], X. H. Xu[a], J. C. Wei[a] and Z. L. Zhou[b]

[a]State Key Laboratory of Nonlinear Mechanics (LNM), Institute of Mechanics, Chinese Academy of Sciences, Beijing, China; [b]306 Institute, The Third Academy of China Aerospace Science and Industry Corporation, Beijing, China

ABSTRACT

We study the difference in the maximum stress on a cylinder surface σ_{max} using the measured surface heat transfer coefficient h_m instead of its average value h_a during quenching. In the quenching temperatures of 200, 300, 400, 500, 600 and 800°C, the maximum surface stress σ_{mmax} calculated by h_m is always smaller than σ_{amax} calculated by h_a, except in the case of 800°C; while the time to reach σ_{max} calculated by h_m (f_{mmax}) is always earlier than that by h_a (f_{amax}). It is inconsistent with the traditional view that σ_{max} increases with increasing Biot number and the time to reach σ_{max} decreases with increasing Biot number. Other temperature-dependent properties also have a small effect on the trend of their mutual ratios with quenching temperatures. Such a difference between the two maximum surface stresses is caused by the dramatic variation of h_m with temperature, which needs to be considered in engineering analysis.

ARTICLE HISTORY
Received 29 September 2015
Accepted 16 December 2015

KEYWORDS
Thermomechanical; ceramics; stress analysis; thermal shock

1. Introduction

The sudden catastrophic reduction in the strength of materials in thermal shock is a long-standing problem in the thermostructural applications of ceramics [1–3]. The mechanism of reduction is traditionally considered to be crack initiation when the stresses induced by a thermal gradient exceed the strength of materials [4,5]. Generally, ceramics are much weaker in tension than in compression, so the maximum tensile stress on the surface of ceramics is of primary interest [6,7].

Based on thermoelastic mechanics, the dimensionless stress on the surface of ceramics with various shapes (the sphere, the plate or the cylinder) during quenching under different thermal shock conditions typically appears as shown in Figure 1 [8–10]. It is clear that each of the curves in Figure 1 has a maximum value σ_{max}. The magnitude of σ_{max} increases with increasing Biot number $\beta = hR/k$, while the time f_{max} when the thermal stress reaches its maximum value decreases with increasing β, where h is the surface heat transfer coefficient

CONTACT F. Song songf@lnm.imech.ac.cn

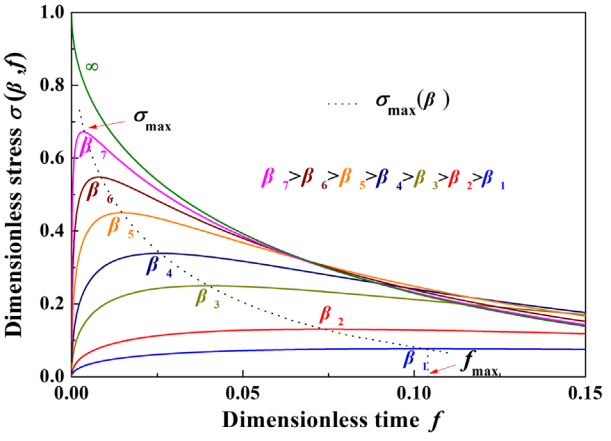

Figure 1. (colour online) Dimensionless stress at the surface of ceramics with various shapes (the sphere, the plate or the cylinder) during quenching under different thermal shock conditions, where the magnitude of the maximum surface stress σ_{max} increases with increasing Biot number β, and the time f_{max} when the thermal stress reaches its maximum value decreases with increasing β.

between the material and the medium, and k and R are the thermal conductivity and the characteristic dimension of the material, respectively. Since it was reported in 1945 by Jaeger, various aspects of σ_{max} have been studied, most importantly the determination of the magnitude and the arrival time of σ_{max} [11,12]. A semi-empirical equation of σ_{max} and β was suggested by Manson and this relation has subsequently been widely used to calculate the resistance of both brittle and ductile materials to crack initiation under cold shock conditions [9,13,14]. In the previous studies, the surface heat transfer coefficient used in the calculation is considered as a constant or an average value. However, the surface heat transfer coefficient largely depends not only on the initial quenching temperature but also on its evolution in quenching media [15,16]. How does the real surface heat transfer coefficient influence the evolution of the surface stress in quenching? Rarely has research focused on this issue, which is of practical importance in engineering analysis. The purpose of this paper is to consider the difference in the maximum surface stress of ceramics arising from the measured surface heat transfer coefficient h_m instead of its average value h_a during quenching.

Firstly, we use h_m and h_a to calculate the thermal fields. Then, we use the thermal fields to calculate the surface stress fields. By comparing the two stress fields, we examine the influences of surface heat transfer coefficient on the magnitude and the arrival time of σ_{max}. At the same time, we also examine the influence of other temperature-dependent physical parameters on $\sigma_{max.}$

2. Methods and calculations

2.1. Surface heat transfer coefficient

We have measured the temperature-dependent surface heat transfer coefficient h_m of Al_2O_3 ceramics quenched from different initial temperatures T_0 into a water bath at room temperature T_∞ [17]. In measurement, the thermocouple instrumented specimens with the

dimensions of 150 mm in height and 50 mm in diameter were first heated at a preset temperature, then they were dropped into a water bath by free fall at 5 cm high from the surface of the water, and the depth of the bath is about 1 m. The specimens touched the wire mesh at the bath bottom while measuring. The details are given elsewhere [17].

The coefficient is a function of the surface temperature T_s of ceramics during the water quench. The measured data are shown in Figure 2 and Table 1. The average value h_a of each surface heat transfer coefficient curve is defined to be

$$h_a = \frac{1}{T_0 - T_\infty} \int_{T_\infty}^{T_0} h(T_s) \mathrm{d}T_s. \tag{1}$$

It is observed that h_m and h_a can be divided into three regions. In the regions I and III, h_a is larger than h_m; while in region II, h_a is less than h_m. In addition, with increasing initial temperature, the range of region I is gradually expanding.

2.2. Temperature distribution

Based on previous experiments [17], we consider an infinite length cylinder of radius R, with a uniform initial temperature T_0. At the initial time, the surface of the cylinder is suddenly exposed to a convective medium with a uniform temperature T_∞, as shown in Figure 3.

The temperature field change in the cylinder $T = T(r, \tau)$ satisfies the equation of heat conduction

$$\frac{\partial T}{\partial \tau} = a \left(\frac{\partial^2 T}{\partial r^2} + \frac{\partial T}{r \partial r} \right), \tag{2}$$

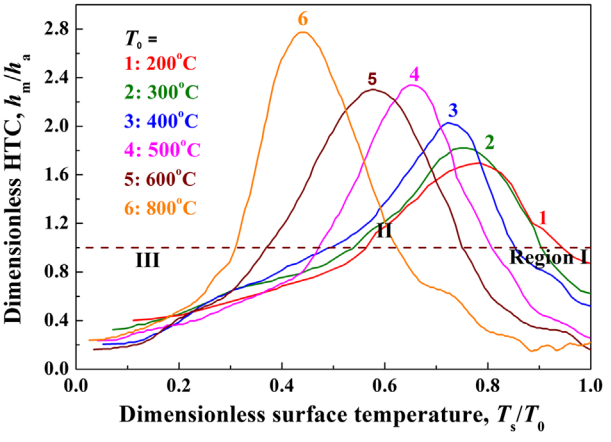

Figure 2. (colour online) Dimensionless surface heat transfer coefficients h_m/h_a for Al_2O_3 ceramic bars quenched into the room temperature water bath from different initial temperatures T_0 are shown as the functions of the transient surface temperatures T_s of the specimens.

Table 1. Average surface heat transfer coefficient h_a for different initial quenching temperatures T_0.

T_0 (°C)	200	300	400	500	600	800
h_a (10^4 W m^{-2} K^{-1})	0.87	0.89	0.93	1.11	1.23	1.05

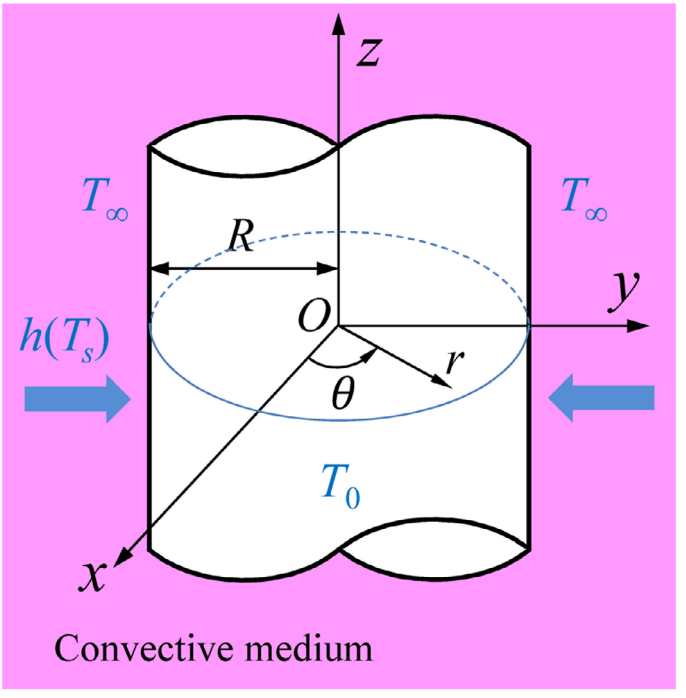

Figure 3. (colour online) An infinitely long cylinder with radius R and initial temperature T_0 is suddenly exposed to a convective medium of temperature T_∞, in which the surface heat transfer coefficient of the materials $h(T_s)$ is the function of surface temperature T_s.

where r is the coordinate with the origin at the centre of the cylinder; τ is time; $a = k/\rho c_p$ is the thermal diffusivity of the material of the cylinder; k, ρ and c_p are the thermal conductivity, the density and the specific heat at constant pressure for the material, respectively.

The initial and boundary conditions that Equation (2) satisfied are written by

$$T(r, 0) = T_0, \tag{3}$$

$$\left.\frac{\partial T}{\partial r}\right|_{r=0} = 0, \tag{4}$$

and

$$-k\left.\frac{\partial T}{\partial r}\right|_{r=R} = h(T - T_\infty). \tag{5}$$

Table 2. Mechanical and thermal parameters of alumina used in calculation.

Young modulus E (GPa) [10]	Poisson's ratio ν [10]	Density ρ (kg m^{-3}) [17]	Heat capacity c (J kg^{-1} K^{-1}) [17]	Thermal conductivity k (W m^{-1} K^{-1}) [17]	Coefficient of thermal expansion α (10^{-6} K^{-1}) [10]
378	0.22	3850	950	20	8.0

Assuming that the properties of the material do not vary with temperature, we can use standard separation-of-variables technique to solve Equation (2) and obtain the following [18]

$$\frac{T-T_0}{T_\infty-T_0}=1-2\sum_{n=1}^{\infty}\frac{J_1(\beta_n)}{\beta_n\left[J_0^2(\beta_n)+J_1^2(\beta_n)\right]}\exp(-\beta_n^2\cdot f)J_0(\beta_n\cdot r^*), \tag{6}$$

where $f = a\tau/R^2$ is the dimensionless time of heat conduction; $r^* = r/R$ stands for the dimensionless coordinate; β_n are the roots of the equation

$$\beta_n\frac{J_1(\beta_n)}{J_0(\beta_n)}=\beta. \tag{7}$$

When the surface heat transfer coefficient h is a function of surface temperature, which satisfies the non-linear boundary conditions, the analytical solution of temperature field cannot be obtained directly from the separation of variables. But if the entire thermal shock process is divided into n small time intervals, and assuming the heat transfer coefficient does not vary with temperature in each interval, we can use the Equation (6) to obtained the temperature field of the first time interval$[0, \Delta f]$ ($\Delta f = 10^{-5}$); and then the obtained temperature was calculated as the initial value of the temperature distribution in the next time interval, so to solve the Equation (6) again we can obtained the temperature field of the second time interval$[\Delta f, 2\Delta f]$; repeating the process described above, we can obtain an approximate numerical solution of the whole process. The mechanical and thermal parameters of alumina used in calculation are given in Table 2.

2.3. Surface stress distribution

According to the theory of thermal stresses [19], we readily write the thermal stress field in the cylinder as

$$\sigma_r(r,\tau)=\frac{\alpha E}{1-\nu}\left[\frac{1}{R^2}\int_0^R(T-T_0)r\mathrm{d}r-\frac{1}{r^2}\int_0^r(T-T_0)r\mathrm{d}r\right], \tag{8}$$

$$\sigma_\theta(r,\tau)=\frac{\alpha E}{1-\nu}\left[\frac{1}{R^2}\int_0^R(T-T_0)r\mathrm{d}r+\frac{1}{r^2}\int_0^r(T-T_0)r\mathrm{d}r-(T-T_0)\right], \tag{9}$$

$$\sigma_z(r,\tau)=\frac{\alpha E}{1-\nu}\left[\frac{2}{R^2}\int_0^R(T-T_0)r\mathrm{d}r-(T-T_0)\right]. \tag{10}$$

Based on Liu's study [12], the maximum tensile thermal stress is the axial stress σ_z on the surface of the cylinder during quenching. Accordingly, in the following, we only focus on σ_z on the surface.

For the convenience of comparing the values of thermal stresses, the dimensionless thermal stress is then defined as [12]

$$\sigma_z^*(r,\tau) = \frac{\sigma_z(r,\tau)\cdot(1-\nu)}{\alpha E(T_\infty - T_0)}. \tag{11}$$

Once the temperature field is determined in each time interval, the transient surface stress can be obtained by Equation (11) in each time interval.

2.4. Finite element model for calculating surface stress

In order to consider the effect of other temperature-dependent properties of alumina on the surface stress, we use the Finite Element (FE) software ANSYS to calculate the surface stress. As shown in Figure 4, the thermal conductivity [20], specific heat [20] and thermal expansion coefficient are strongly temperature-dependent in the range 20–800 °C [21]. But the Young's modulus, Poisson's ratio and density is regarded as temperature-independent [22], as shown in Table 2.

3. Results and discussion

Using the data of h_m and h_a, the temperature fields occur in the cylinder for different initial quenching temperatures (different Biot numbers) during cooling are readily calculated by solving Equation (6), as shown in Figure 5(a)–(d). Comparing the two temperature fields, we find that for all the quenching temperatures, the temperature fields in the position of the axis, the middle layer and the surface of cylindrical specimen, calculated by h_a are substantially lower than that by h_m, except the initial period in the surface temperature field of the cylinder, as shown in the enlarged pictures.

We can see that, initially, the surface temperature T_{sa} calculated with h_a drops more sharply than the surface temperature T_{sm} with h_m, which means the amount of heat transferred in this period is estimated to be greater than in the calculation based on h_m, as h_a is larger than h_m in region I. With increasing initial temperature, the time period when T_{sa} is lower than T_{sm} becomes longer, because the range of the region I is gradually expanding with increasing initial temperature. Then, T_{sa} gradually becomes higher than T_{sm} as h_a is less than h_m in region II. Finally, T_{sa} become lower than T_{sm} again as h_a is

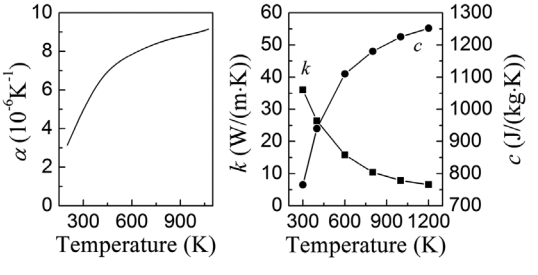

Figure 4. Graphs of the thermal conductivity k [20], the specific heat c [20] and the coefficient of thermal expansion α [21] of Al_2O_3 ceramics vs. temperature.

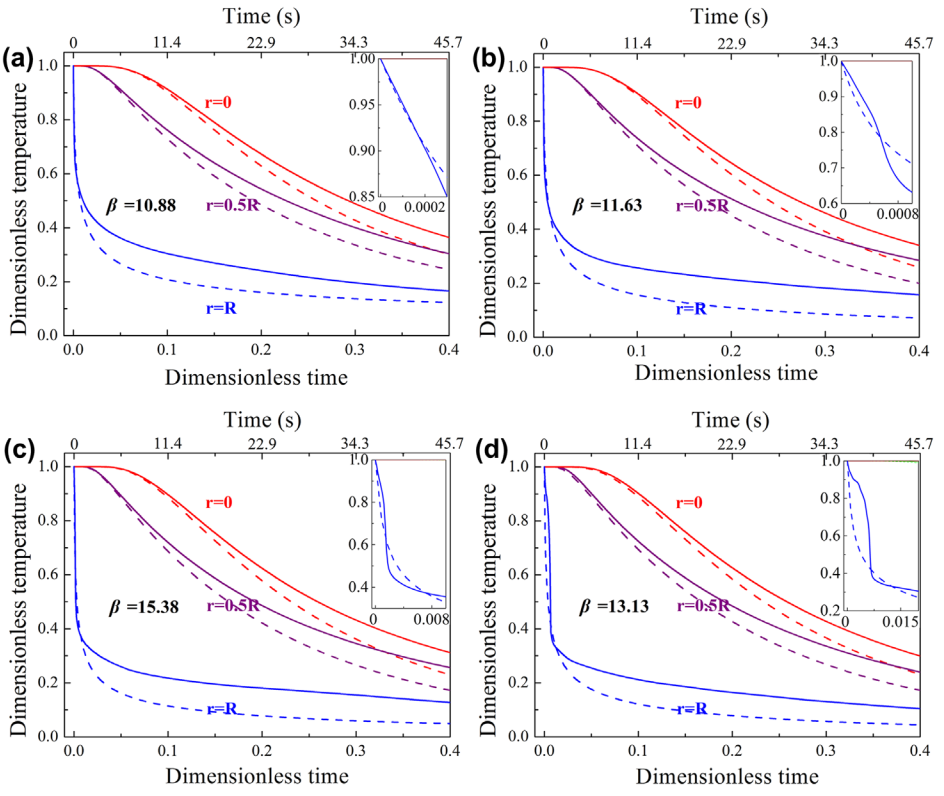

Figure 5. (colour online) Comparison between the temperature fields obtained by the measured heat transfer coefficient (the solid line) and the average heat transfer coefficient (the dotted line), for initial quenching temperature T_0 = (a) 200 °C, (b) 400 °C, (c) 600 °C, (d) 800 °C, where $r = 0, 0.5R, R$ represent the position of the axis, the middle layer and the surface of the cylindrical specimen, respectively.

larger than h_m in region III, which made the temperature fields calculated by h_a lower than that by h_m in the later time.

The thermal stress fields calculated by h_m and h_a for different initial quenching temperatures are shown in Figure 6(a)–(d). Referring to the insets in Figure 6, initially, the surface stress σ_{sm} calculated with h_m is slightly lower than the surface stress σ_{sa} calculated by h_a, and the time period when σ_{sm} is lower than σ_{sa} becomes longer with increasing initial temperature. Then, σ_{sm} become higher than σ_{sa}. Finally, σ_{sm} become lower than σ_{sa} again, corresponding to the different temperature profiles in Figure 5.

To indicate the influences of the temperature-dependent heat transfer coefficient on the magnitude and the arrival time of σ_{max}, the comparison between the thermal stresses on the surface obtained by h_m and h_a for different initial quenching temperatures is shown in Figure 7. When using data of h_a, we can find that, the magnitude of the maximum surface stress σ_{amax} are $\sigma_{600\,°C} > \sigma_{500\,°C} > \sigma_{800\,°C} > \sigma_{400\,°C} > \sigma_{300\,°C} > \sigma_{200\,°C}$, and that the time to reach the maximum surface stress f_{amax} are $f_{600\,°C} < f_{500\,°C} < f_{800\,°C} < f_{400\,°C} < f_{300\,°C} < f_{200\,°C}$, respectively. It is consistent with traditional view that f_{max} decreases with increasing β and σ_{max} increases with increasing β [8–10]. While using data of h_m, the magnitude of the maximum surface stress σ_{mmax} are $\sigma_{800\,°C} > \sigma_{600\,°C} > \sigma_{500\,°C} > \sigma_{400\,°}$

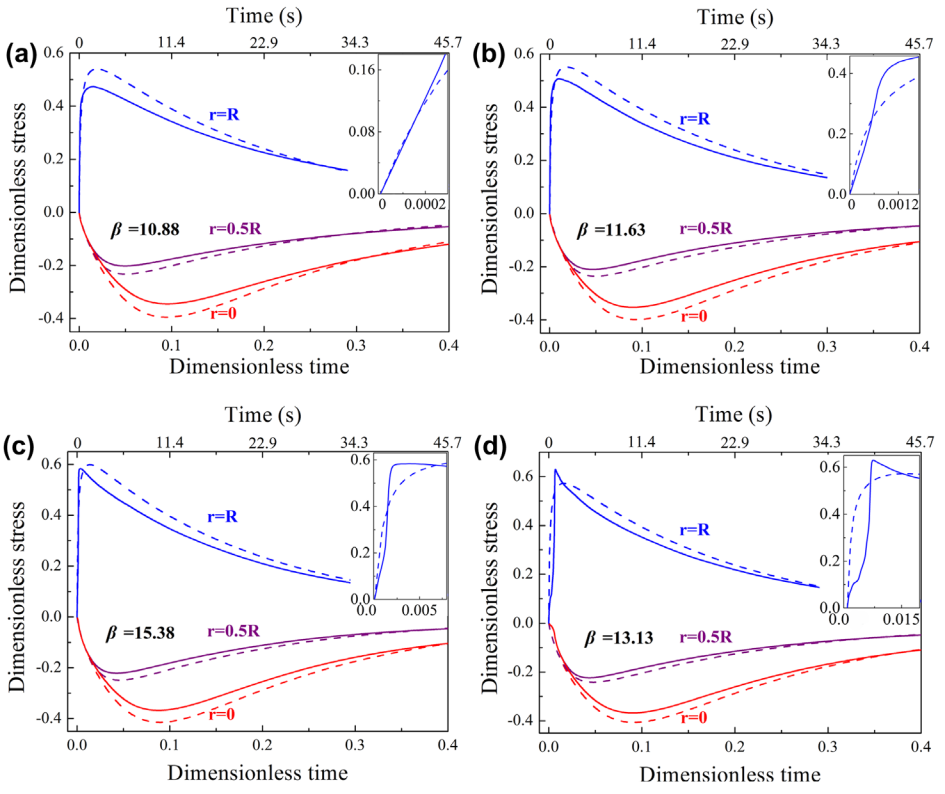

Figure 6. (colour online) Comparison of the thermal stress fields obtained by the measured heat transfer coefficient (the solid line) and the average heat transfer coefficient (the dotted line), for initial quenching temperature T_0 = (a) 200 °C, (b) 400 °C, (c) 600 °C, (d) 800 °C, where $r = 0, 0.5R, R$ represent the position of the axis, the middle layer and the surface of cylindrical specimen, respectively.

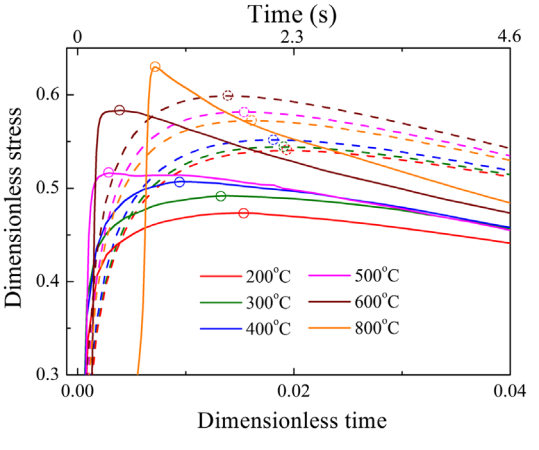

Figure 7. (colour online) Comparison between the thermal stress at the surface obtained by the measured heat transfer coefficient (the solid lines) and the average heat transfer coefficient (the dotted lines), for different initial quenching temperatures. The marks represent the maximum stresses.

$_{C} > \sigma_{300\,°C} > \sigma_{200\,°C}$, and the time to reach the maximum surface stress f_{mmax} are $f_{500\,°C} < f_{600\,°C} < f_{800\,°C} < f_{400\,°C} < f_{300\,°C} < f_{200\,°C}$, respectively. Therefore, when the initial quenching temperature $T_0 \leq 400$ °C, it follows the traditional view before; while in the case of $T_0 > 400$ °C, it does not obey this rule.

In addition, we find that in all the quenching temperatures, the magnitude of σ_{max} calculated by h_m is always lower than that by h_a, except $T_0 > 600$ °C, as listed in Table 3. The ratio $(\sigma_{amax} - \sigma_{mmax})/\sigma_{mmax}$ decreases from 14.1% at 200°C to −9.1% at 800 °C and the change is not great. Thus, from the point of view of stress magnitude, the traditional usage of h_a instead of h_m is roughly reasonable during the ceramic quenching. Further, we find that in all the quenching temperatures, the time to reach the maximum stress calculated by h_m is always earlier than that by h_a, as listed in Table 4. The ratio $(f_{amax} - f_{mmax})/f_{mmax}$ increases from 22.4% at 200°C to 437.9% at 500°C, and the change is substantially greater than that in the magnitude of σ_{max}. Thus, when the time factor is important, such as short-time thermal shock [23], it is not a good strategy to use h_a instead of h_m.

Considering the temperature-dependent properties of thermal conductivity, specific heat and thermal expansion coefficient, a comparison between the thermal stresses on the surface obtained by h_m and h_a for different initial quenching temperatures is shown in Figure 8. When using data of h_a, the magnitude of the maximum surface stress σ_{amax} are $\sigma_{800\,°C} > \sigma_{600\,°C} > \sigma_{500°C} > \sigma_{400°C} > \sigma_{300°C} > \sigma_{200°C}$, and the time to reach the maximum surface stress f_{amax} are $f_{600°C} < f_{800°C} < f_{500°C} < f_{400°C} < f_{200°C} < f_{300°C}$, respectively. While using data of h_m, the magnitude of the maximum surface stress σ_{mmax} are $\sigma_{800°C} > \sigma_{600°C} > \sigma_{500°C} > \sigma_{400°C} > \sigma_{300°C} > \sigma_{200°C}$, and the time to reach the maximum surface stress f_{mmax} are $f_{500°C} < f$

Table 3. Magnitude of the maximum surface stress σ_{max} calculated by the measured surface heat transfer coefficient (σ_{mmax}) and the average surface heat transfer coefficient (σ_{amax}), for different initial quenching temperatures T_0.

T_0 (°C)	200	300	400	500	600	800
σ_{amax}	0.5403	0.5441	0.5517	0.5816	0.5987	0.5722
σ_{mmax}	0.4735	0.4919	0.5070	0.5162	0.5832	0.6295
$(\sigma_{amax} - \sigma_{mmax})/\sigma_{mmax}$	14.1%	10.6%	8.8%	12.7%	2.7%	−9.1%

Table 4. Time to reach the maximum stress f_{max} calculated by the measured surface heat transfer coefficient (f_{mmax}) and the average surface heat transfer coefficient (f_{amax}), for different initial quenching temperatures T_0.

T_0 (°C)	200	300	400	500	600	800
f_{amax}	0.0191	0.0190	0.0181	0.0156	0.0138	0.0164
f_{mmax}	0.0156	0.0138	0.0095	0.0029	0.0040	0.0071
$(f_{amax} - f_{mmax})/f_{mmax}$	22.4%	37.7%	90.5%	437.9%	245.0%	131.0%

Table 5. In the case of FE analyses using the temperature dependent thermal properties, the magnitude of the maximum surface stress σ_{max} calculated by the measured surface heat transfer coefficient (σ_{mmax}) and the average surface heat transfer coefficient (σ_{amax}), for different initial quenching temperatures T_0.

T_0 (°C)	200	300	400	500	600	800
σ_{amax}	0.5844	0.6105	0.6505	0.7177	0.7571	0.7832
σ_{mmax}	0.5275	0.5557	0.6199	0.6820	0.7710	0.8711
$(\sigma_{amax} - \sigma_{mmax})/\sigma_{mmax}$	11.2%	9.9%	4.9%	5.2%	−1.8%	−10.1%

Table 6. In the case of FE analyses using the temperature dependent thermal properties, the time to reach the maximum stress f_{max} calculated by the measured surface heat transfer coefficient (f_{mmax}) and the average surface heat transfer coefficient (f_{amax}), for different initial quenching temperatures T_0.

T_0 (°C)	200	300	400	500	600	800
f_{amax}	0.0156	0.0203	0.0142	0.0115	0.0105	0.0109
f_{mmax}	0.0124	0.0095	0.0099	0.0021	0.0023	0.0051
$(f_{amax} - f_{mmax})/f_{mmax}$	25.8%	113.7%	42.6%	455.1%	348.5%	113.5%

$_{600°C} < f_{800°C} < f_{300°C} < f_{400°C} < f_{200°C}$, respectively. It is indicated that they do not follow the traditional view anymore. Therefore, the other temperature-dependent properties have a certain effect on the magnitude and the arrival time of σ_{max}. However, the effect on the trend of their mutual ratios with quenching temperatures is small, as listed in Tables 3–6. The ratio $(\sigma_{amax} - \sigma_{mmax})/\sigma_{mmax}$ decreases from 11.2% at 200°C to −10.1% at 800°C and the ratio $(f_{amax} - f_{mmax})/f_{mtmax}$ increases from 25.8% at 200°C to 455.1% at 500°C. We believe that the cause of this difference between the two maximum surface stresses is the features of h_m, which first increases to reach a maximum value and afterwards decreases as the surface temperature decreases. Note that the changes with temperature in other properties (Young's modulus, Poisson's ratio and density) are much smaller, and in this study they have been ignored.

In addition, Cheng used a method similar to us to investigate the surface heat transfer coefficient h of steel cylinders with the dimensions of 60 mm in height and 20 mm in diameter [24], which is 0.4 of our samples in height and diameter, respectively. We find that the feature of h in Cheng's study is similar to us. Thus, our results may be also valid for the specimens with similar dimensions and shapes. To provide more precise instructions to engineering analysis, further studies should be conducted to identify how the surface heat transfer coefficient changes with the size.

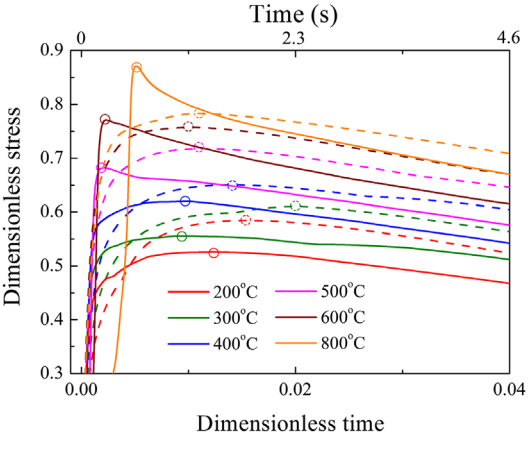

Figure 8. (colour online) In the case of FE analyses using the temperature-dependent thermal properties, the comparison between the thermal stress at the surface obtained by the measured heat transfer coefficient (the solid lines) and the average heat transfer coefficient (the dotted lines), for different initial quenching temperatures. The marks represent the maximum stresses.

4. Conclusions

When the initial quenching temperature is $T_0 \leq 400°C$, the maximum surface stress σ_{max} and the time to reach the maximum surface stress f_{max} calculated by measured surface heat transfer coefficient h_m are consistent with the traditional view that σ_{max} increases with increasing Biot number and f_{max} decreases with increasing Biot number; while $T_0 > 400°C$, it does not obey this rule. However, in the case of other temperature-dependent physical parameters, they do not follow the traditional view anymore. As a result, using average surface heat transfer coefficient h_a instead of h_m will introduce a small error in the magnitude of σ_{max}, however, the error introduces in the arrival time of σ_{max} is significant.

Acknowledgement

This work is supported by the National Natural Science Foundation of China [grant number 11102208], [grant number 11232013], [grant number 11472285] and [grant number 11572326].

Disclosure statement

No potential conflict of interest was reported by the authors.

References

[1] R. Danzer, T. Lube, P. Supancic, and R. Damani, *Fracture of ceramics*, Adv. Eng. Mater. 10 (2008), p. 275–298.
[2] B. Bourdin, J.J. Marigo, C. Maurini, and P. Sicsic, *Morphogenesis and propagation of complex cracks induced by thermal shocks*, Phys. Rev. Lett. 112 (2014), p. 014301.
[3] F. Song, S.H. Meng, X.H. Xu, and Y.F. Shao, *Enhanced thermal shock resistance of ceramics through biomimetically inspired nanofins*, Phys. Rev. Lett. 104 (2010), p. 125502.
[4] W.D. Kingery, *Factors affecting thermal stress resistance of ceramic materials*, J. Am. Ceram. Soc. 38 (1955), p. 3–15.
[5] J. Li, F. Song, and C.P. Jiang, *Direct numerical simulations on crack formation in ceramic materials under thermal shock by using a non-local fracture model*, J. Eur. Ceram. Soc. 33 (2013), p. 2677–2687.
[6] W.D. Kingery, H.K. Bowen, and D.R. Uhlmann, *Introduction to Ceramics*, Wiley, New York, 1976, p. 821.
[7] Q.N. Liu, F. Song, S.H. Meng, and C.P. Jiang, *Universal Biot number determining stress duration and susceptibility of ceramic cylinders to quenching*, Philos. Mag. 90 (2010), p. 1726–1732.
[8] J.C. Jaeger, *LI. On thermal stresses in circular cylinders*, Philos. Mag. 36 (1945), p. 418–428.
[9] S.S. Manson, *Behavior of materials under conditions of thermal stress*, NACA TN 2933, (1953), p. 270.
[10] Y.F. Shao, Q.N. Liu, H.J. Tian, Z.K. Lin, X.H. Xu, and F. Song, *Dimension limit for thermal shock failure*, Philos. Mag. 94 (2014), p. 2647–2655.
[11] T.J. Lu and N.A. Fleck, *The thermal shock resistance of solids,* Acta Mater. 46 (1998), p. 4755–4768.
[12] F. Song, Q.N. Liu, S.H. Meng, and C.P. Jiang, *A universal Biot number determining the susceptibility of ceramics to quenching*, EPL (Europhys. Lett.) 87 (2009), p. 54001.
[13] H.G. Baron, *Thermal shock and thermal fatigue*, in *Thermal Stresses*, P.P. Benham and R. Hoyle, eds., Sir Isaac Pitman & Sons Ltd., London, 1964, p. 182.
[14] S.S. Manson and T.J. Dolan, *Thermal stress and low-cycle fatigue*, J. Appl. Mech. 33 (1966), p. 957.
[15] P.F. Becher, *Effect of water bath temperature on the thermal shock of Al_2O_3*, J. Am. Ceram. Soc. 64 (1981), p. C17–C18.

[16] J.P. Singh, Y. Tree, and D.P.H. Hasselman, *Effect of bath and specimen temperature on the thermal stress resistance of brittle ceramics subjected to thermal quenching*, J. Mater. Sci. 16 (1981), p. 2109–2118.
[17] Z.L. Zhou, F. Song, Y.F. Shao, S.H. Meng, C.P. Jiang, and J. Li, *Characteristics of the surface heat transfer coefficient for Al_2O_3 ceramic in water quench*, J. Eur. Ceram. Soc. 32 (2012), p. 3029–3034.
[18] P.J. Schneider, *Conduction Heat Transfer*, Addison-Wesley Publishing Company Inc, Cambridge, 1955, p. 255.
[19] B.A. Boley and J.H. Weiner, *Theory of Thermal Stresses*, Wiley, New York, 1960, p. 302.
[20] T.L. Bergman, A.S. Lavine, F.P. Incropera, and D.P. Dewitt, *Fundamentals of Heat and Mass Transfer*, Wiley, Hoboken, 2011, p. 987.
[21] D.L. Jiang, L.T. Li, S.X. Ouyang, and J.L. Shi, *China Materials Engineering Canon*, Chemical Industry Press, Beijing, 2006, p. 35.
[22] C.P. Jiang, X.F. Wu, J. Li, F. Song, Y.F. Shao, X.H. Xu, and P. Yan, *A study of the mechanism of formation and numerical simulations of crack patterns in ceramics subjected to thermal shock*, Acta Mater. 60 (2012), p. 4540–4550.
[23] J. Absi and J.C. Glandus, *Improved method for severe thermal shocks testing of ceramics by water quenching*, J. Eur. Ceram. Soc. 24 (2004), p. 2835–2838.
[24] H.M. Cheng, H.G. Wang, and T.L. Chen, *Solution of heat conduction inverse problem for steel 45 during quenching*, Acta Metall. Sinica 33 (1997), p. 467–472.